25th International Conference on Fracture and Structural Integrity

Multiaxial fatigue behavior of additive manufactured Ti-6Al-4V under in-phase stresses

Danilo A. Renzo[a], Emanuele Sgambitterra[a], Pietro Magarò[a], Franco Furgiuele[a], Carmine Maletta[a, *], Carlo Biffi[b], Jacopo Fiocchi[b], Ausonio Tuissi[b]

[a]DIMEG - Dept. of Mechanical, Energy and Management Engineering, University of Calabria, 87036 Rende, Italy
[a]CNR-ICMATE - Lecco, 23900, Italy

Abstract

The development and application of additive manufacturing (AM) technologies is constantly increasing. However, in many applications, AM parts are subjected to multiaxial loads, arising from operating conditions and/or complex geometries. These make AM components serious candidates for crack initiation and propagation mechanisms. Therefore, a deep understanding of the multiaxial fatigue behavior of AM parts is essential in many applications where durability and reliability are core issues. In this study, multiaxial fatigue of Ti6Al4V thin-walled tubular specimens, made by Selective Laser Melting (SLM) process, was investigated by combined axial-torsional loads. Infrared thermography (IR) was also used to investigate the temperature evolution during fatigue tests. Results highlighted different damage mechanisms and failure modes in the low- and high-cycle fatigue regimes.

Keywords: Multiaxial fatigue; In-phase stresses; Select Laser Melting; Additive Manufacturing; Ti-6Al-4V; Infrared Thermographic technique.

1. Introduction

Titanium alloys, and in particular the Ti6Al4V system, have become very attractive engineering materials in last years, due to their high strength and fracture toughness, low density, good corrosion resistance and biocompatibility

---

* Corresponding author. Tel.: +39 0984 494662; fax: +39 0984 496473.
  E-mail address: carmine.maletta@unical.it

(Donachie 2000, Cui 2011). In fact, thanks to these excellent properties, Ti6Al4V is largely used in several high demanding applications in aerospace, automotive, marine and biomedical fields (Inagaki 2014, Boyer 1996, Singh 2017, Uhlmann 2015).

The most conventional way to manufacture Ti6Al4V products is based on forging, casting and rolling processes, usually followed by machining, in order to obtain complex shaped components. However, these are expensive and time consuming processes and they always generate large amount of material waste (Huang 2016, Lütjering 2007).

In this landscape, additive manufacturing (AM) technology, that works adding materials in a layer-by-layer fashion starting from a CAD model, can represent a good challenge to fabricate Ti6Al4V products with geometric complexities (Uhlmann 2015, Huang 2016). Compared to most traditional manufacturing methods, the great advantage of AM is the freeform fabrication capability of complex components, directly from feedstock materials without involving secondary machining processes to get the desired geometry.

Among the different additive manufacturing technologies, select laser melting (SLM) is increasingly used in several engineer applications, especially when dealing with titanium components. It uses a high power density laser to melt metallic powders of Ti6Al4V. However, due to the highly localized heat input and short interaction time, large temperature gradients and high cooling rates are involved during the process (Katinas 2018, Liu 2018), affecting the final microstructure of the material and generating high residual stresses. Furthermore, unavoidable defects are usually generated by the AM processes reducing the mechanical performance and fatigue resistance (Strantza 2016, Biswas 2012, Beretta 2017).

In addition, it is important to point out that AM manufacturing process generates some anisotropy caused by the layer by layer deposition, i.e. mechanical proprieties result direction-dependent (Carrol 2015). In fact, it was shown that the tensile strength along the build direction is slightly lower than the in-plane ones. In addition, these anisotropies are expected to play significant effects on the fatigue response of AM parts (Liu 2019), especially when dealing with multiaxial conditions.

An extensively review on fatigue properties of Ti6Al4V AM components, under axial cyclic conditions, was made by Li et al. (2016). It was shown that AM materials always have shorter lives compared to the wrought material. Internal defects, residual stresses, and surface condition are key factors for fatigue damage of AM materials. The effects of internal defects and residual stresses in Ti6Al4V AM specimens were directely investigated by Edwards et al. (2014), under uniaxial fatigue conditions. They found a marked reduction in the fatigue strength (around 75%) with respect to the wrought material. Similar results were obtained by Wycisk et al. (2014) and Fatemi et al. (2017), which analyzed the effects of surface conditions under axial and torsional fatigue conditions, respectively.

However, most of the literature studies are focused on the uniaxial fatigue properties of Ti6Al4V AM, even if multiaxial loadings represent the most typical condtions in real complex shaped components. This is of major concern due to the material anisotropies and to the lack of knowledeges about equivalent stress criteria. Multiaxial fatigue behavior of Ti6Al4V was firstly investigated in (Fatemi et al., 2017), by systematic comparison between AM and wrought samples. Results revealed that internal porosity/defects or near surface defects cause marked reductions in the fatigue properties of AM specimens.

However, systematic studies should be carried out, for a deeper understanding of key damage mechanisms in Ti6Al4V AM parts, as well as to develop effective and reliable predictive models.

In this study the multiaxial fatigue on Ti6Al4V AM samples made by Selective Laser Melting (SLM) was investigated. Multiaxial fatigue conditions were obtained combining axial and torsional in-phase proportional loads. Infrared Thermography (IR) technique was also used to investigate the thermal evolution during the fatigue tests. Results highlighted different damage mechanisms and failure modes in the low- and high-cycle fatigue regimes.

2. Material and methods

2.1. Materials and manufacturing process

Thin-walled tubular specimens with wall thickness of 0.85 mm were designed based on the ASTM Standard E2207. The geometry of the specimen is shown in Fig. 1.
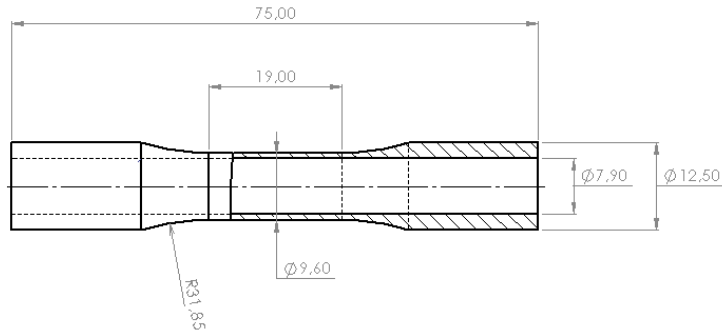
Figure 1. Thin-walled tubular specimen geometry with nominal dimensions.

AM samples were made by SLM process (AM400 Fro Renishaw), by using spherical micrometric powder of Ti6Al4V and the process parameters are listed in Table 1.

Table 1. SLM process parameters.

Power	Exposure time	Layer thickness	Scanning strategy	Spot size	Point distance
400 W	60 μs	60 μm	Meander	65 μm	80 μm

The specimens were heat treated at 850 °C for 1 hour in vacuum followed by cooling in flowing air atmosphere. AM specimens were subsequently machined and polished (diamond compund: 9 μm and 3 μm), at both outer and inner surfaces, before testing. The resultaning surface roughness R_a was equal to 0.2 μm.

Monotonic tensile and torsional tests, under displacement and rotation-controlled mode, respectively, were performed to measure the static mechanical properties AM samples. Results are shown in Figs. 2. In particular, Fig. 2.a shows the tensile stress-strain response together with the main axial mechanical parameter, i.e. elastic modulus E=108.7 GPa, yield stress σ_y=860 MPa and ultimate stress σ_{ult}=948 MPa. Figure 2.b shows the shear stress-strain response together with significant mechanical parameter, i.e. shear modulus G=40 GPa, shear yield stress τ_y=562 MPa and shear ultimate stress τ_{ult}=826 MPa.
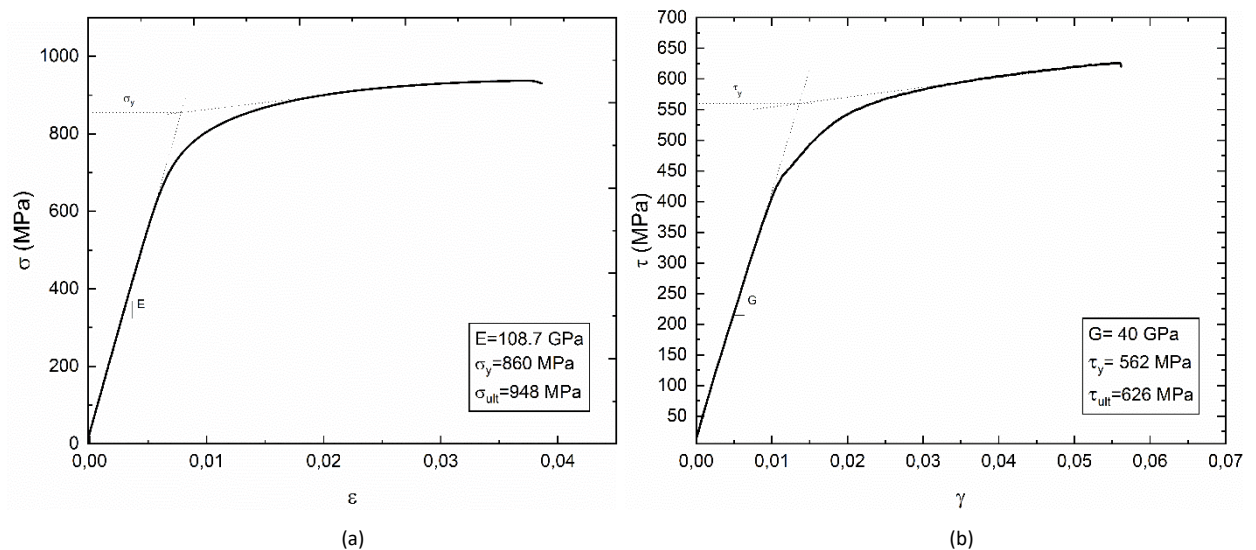

Figure 2. Monotonic stress-strain curves of AM specimen under (a) tension and (b) torsion loading conditions.

2.2. Fatigue testing

Multiaxial fatigue testing conditions were obtained combining axial-torsion in-phase loads. In this study, the following in-phase stresses ratio was selected:

$$\frac{\tau_{xy}}{\sigma_y} = \frac{\sqrt{3}}{3}$$ (1)

A schematic representation of the applied loading conditions is shown in Figs. 3. In particular, Fig. 3.a reports the time evolution of the axial and torsional stress components, Fig. 3.b shows the load path (τ vs σ) and Fig. 3.c illustrates the load ratio vs time (τ/σ vs t).
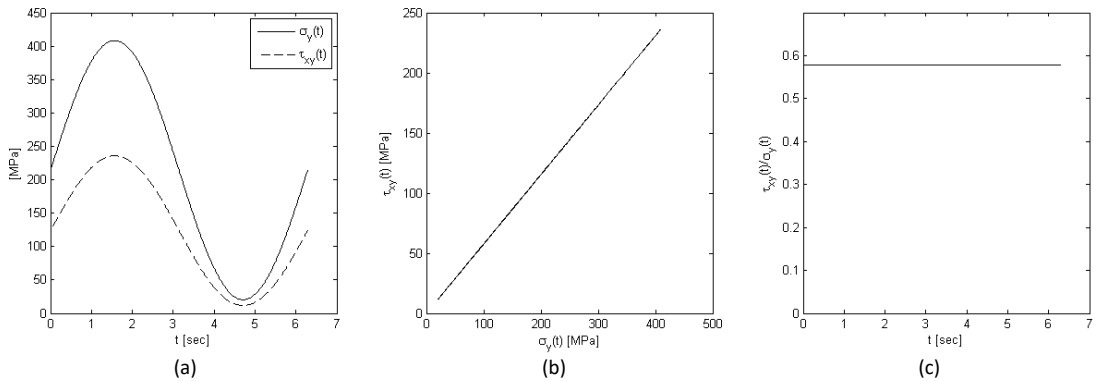

Figure 3: (a) Wave In-phase axial and torsion stress time for 55% of S_{ut}; (b) In-phase load path; (c) In-phase constant stresses ratio.

The multiaxial fatigue tests were carried out using an axial-torsion electrodynamic testing machine (Instron, ElectroPulse E10000) with an axial and torsional capacity of 10 kN and 100 Nm, respectively. All tests were performed in load control ($R=\sigma_{min}/\sigma_{max}=\tau_{min}/\tau_{max}=0.05$) at environmental temperature and a sinusoidal waveform was used. The maximum and minimum values of tensile and tangential stress were evaluated using the von Mises equivalent stress criterion. Loading conditions for the multiaxial fatigue tests are summarized in Table 2, in terms of axial stress amplitude (σ_a), axial mean stress (σ_m), shear stress amplitude (τ_a) the shear mean stress (τ_m). The table also reports the maximum equivalent stress ($\sigma_{max,eq}$) together wih the ratio with respect to the ultimate tensile stress ($\sigma_{max,eq}/S_{ut}$)

Table 2. Multiaxial fatigue test conditions.

Test contition #1	σ_a (MPa)	σ_m (MPa)	τ_a (MPa)	τ_m (MPa)	$\sigma_{max,eq}$ (MPa)	$\sigma_{max,eq}/S_{ut}$
1	194	215	112	124	580	0.61
2	176	195	102	112	524	0.55
3	141	156	81	90	420	0.44
4	123	136	71	79	367	0.38
5	106	117	61	68	315	0.33
6	88	97	51	56	262	0.27
7	64	71	37	41	190	0.20

Infrared thermographic analyses were conducted using an IR camera (FLIR, A615), with a resolution of 320x256 pixels, and results were analyzed by a commercial IR imaging software (FLIR, Tools+). The surface of the samples was painted black to obtain an emissivity of about 0.95. The temperature of the specimens surface was recorded and analyzed during fatigue test.

3. Results and discussion

Results obtained from the experiments are presented in Table 3, whereas the corresponding fatigue resistance curve, in terms of equivalent stress amplitude $\sigma_{a,eq}$ as a function of the number of cycles to failure, is shown in Fig. 4.

Table 3. Multiaxial fatigue test results

ID sample	$\sigma_{a,eq}$ (MPa)	Cycles to failure (N_f)
P1	274	16159
P2	249	26574
P3	199	56591
P4	199	87316
P5	174	156630
P6	150	95006
P7	125	393363
P8	91	2000000

Results showed that, at the first stage the crack nucleates and growth on the maximum shear plane, $\alpha=16.44°$. When the crack became longer, mode I crack propagation is predominant and, therefore, there is a deviation of the crack path from the maximum shear plane to the maximum principal stress plane until the complete failure of the sample.
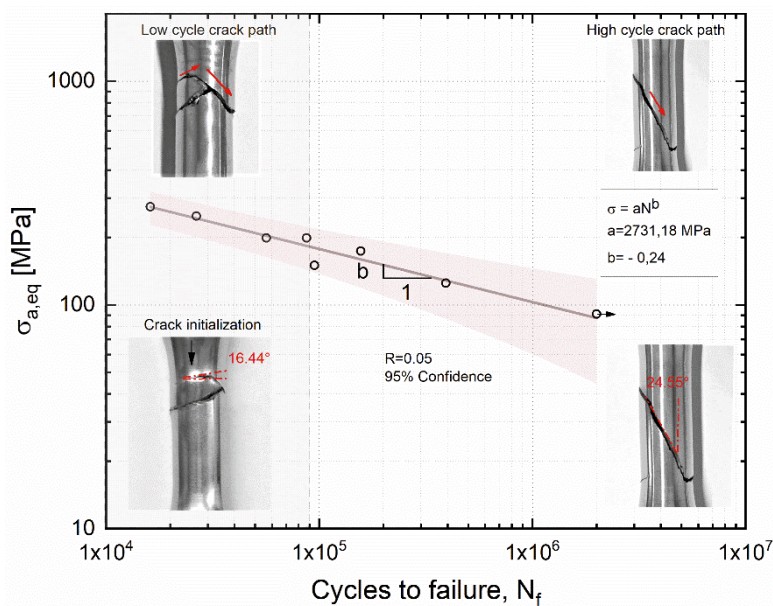

Figure 4. Multiaxial fatigue test result of AM specimen under in-phase load condition.

IR images of the specimens during fatigue tests were uased to analize the failure modes of the samples under both low- and high-cycle fatigue, and to better analyze the crack path evolution, as previously discussed. In addition, local temperature increase were observed in the crack formation zone due to the development of plastic strain.

The time profile of the temperature, obtained from the IR images, shows the typical trend of the T-N curve (Fig. 5) that is characterized by three phases: an initial increase of the temperature (phase I), an approximately constant value of temperature (Phase II) and a sudden temperature increase as soon as the plastic deformations become relevant, bringing the test specimen to fracture (phase III).
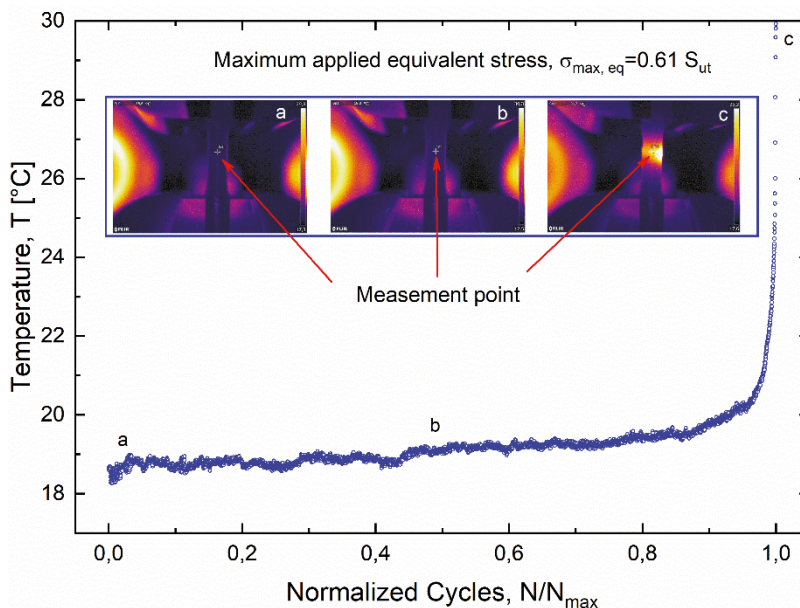
Fig. 5 Evolution of surface temperature of sample P1 during multiaxial fatigue test.

Conclusions

In this study the multiaxial fatigue behavior of thin walled Ti6Al4V AM specimens under proportional in-phase stress conditions was analyzed. It was found that crack direction changes during crack propagation, i.e. it is close to the maximum shear plane for small cracks and approaches the maximum tensile stress direction for long cracks. Furthermore, infrared investigations were carried out to analyzed the evolution of surface temperature during fatigue test. The results provide an initial understanding of multiaxial fatigue behavior of Ti6Al4V AM samples under in-phase loading conditions. Further studies have been undertaken for a deeper analysis of multiaxial fatigue properties of Ti6Al4V AM samples under both proportional and non-proportional loads.

References

ASTM E2207. Standard Practice for Strain-Controlled Axial-Torsional Fatigue Testing with Thin-Walled Tubular Specimens

Beretta, S., Romano, S., 2017. A comparison of fatigue strength sensitivity to defects for materials manufactured by AM or traditional processes, International Journal of Fatigue 94 178-191.

Biswas, N., Ding, J.L., Balla, V.K., Field, D.P., Bandyopadhyay, A., 2012. Deformation and fracture behavior of laser processed dense and porous Ti6Al4V alloy under static and dynamic loading, Materials Science and Engineering A 549 213-221.

Boyer, R.R., 1996. An overview on the use of titanium in the aerospace industry. Materials Science and Engineering A 213 (1) 103-114.

Carroll, B.E., Palmer, T.A., Beese, A.M., 2015. Anisotropic tensile behavior of Ti-6Al-4V components fabricated with directed energy deposition additive manufacturing. Acta Materialia, volume 87, pag. 309-320.

Cui, C., Hu, B., Zhao, L., Liu, S., 2011. Titanium alloy production technology, market prospectsand industry development, Materials & Design, 32 (3) 1684-1691.

Donachie, M.J., 2000. Titanium: A Technical Guide, second ed. ASM International, Materials Park, OH.

Edwards, P., Ramulu, M., 2014. Fatigue performance evaluation of selective laser melted Ti–6Al–4V. Materials Science and Engineering A 598:327-37.

Fatemi, A., Molaei, R., Sharifimehr, S., Shamsaei, N., Phan, N., 2017. Torsional fatigue behavior of wrought and additive manufactured Ti-6Al-4V by powder bed fusion including surface finish effect. International Journal of Fatigue 99:187-201.

Fatemi, A., Molaei, R., Sharifimehr, S., Shamsaei, N., Phan, N., 2017. Multiaxial fatigue behavior of wrought and additive manufactured Ti-6Al-4V including surface finish effect. International Journal of Fatigue 100:347-366.

Huang, R., Riddle, M., Graziano, D., Warren, J., Das, S., Nimbalkar, S., Cresko, J., Masanet, E., 2016. Energy and emissions saving potential of additive manufacturing: the case of lightweight aircraft components. Journal of Cleaner Production 135 1559-1570.

Inagaki, I., Takechi, T., Shirai, Y., Ariyasu, N., 2014. Application and features of titanium for the aerospace industry. Nippon Steel & Sumitomo Metal Technical Report, pp. 22-27.

Katinas, C., Liu, S., Shin, Y.C., 2018. Self-sufficientmodeling of single track deposition of Ti-6Al-4V with the prediction of capture efficiency. Journal of Manufacturing Science and Engineering 141 (1) (011001-011001-10).

Li, P., Warner, D., Fatemi, A., Phan, N., 2016. Critical assessment of the fatigue performance of additively manufactured Ti-6Al-4V and perspective for future research. International Journal of Fatigue 85:130-43.

Liu, S., Shin, Y.C., 2018. Simulation and experimental studies on microstructure evolution of resolidified dendritic TiCx in laser direct deposited Ti-TiC composite. Materials & Design 159 212-223

Liu, S., Shin, Y.C., 2019. Additive manufacturing of Ti6Al4V alloy: A review. Materials and Design 164 107552.

Lütjering, G., Williams, J.C., 2007. Titanium, second ed. Springer, New York.

Singh, P., Pungotra, H., Kalsi, N.S., 2017. On the characteristics of titanium alloys for the aircraft applications. Materials Today Proceedings 4 (8) 8971-8982.

Strantza, M., Vafadari, R., De Baere, D., Vrancken, B., Van Paepegem, W., Vandendael, I., Terryn, H., Guillaume, P., Van Hemelrijck, D., 2016. Fatigue of Ti6Al4V structural health monitoring systems produced by selective laser melting. Materials (Basel) 9 (2).

Uhlmann, E., Kersting, R., Klein, T.B., Cruz, M.F., Borille, A.V., 2015. Additive manufacturing of titanium alloy for aircraft components. Procedia CIRP 35 55-60.

Wycisk, E., Solbach, A., Siddique, S., Herzog, D., Walther, F., Emmelmann, C., 2014. Effects of defects in laser additive manufactured Ti-6Al-4V on fatigue properties. Physics Procedia 56:371-8.